

# Solar Activity Parameters and Associated Forbush Decreases During the Minimum Between Cycles 23 and 24 and the Ascending Phase of Cycle 24

D. Lingri<sup>1</sup> · H. Mavromichalaki<sup>1</sup> · A. Belov<sup>2</sup> ·  
E. Eroshenko<sup>2</sup> · V. Yanke<sup>2</sup> · A. Abunin<sup>2</sup> · M. Abunina<sup>2</sup>

Received: 19 October 2015 / Accepted: 6 February 2016  
© Springer Science+Business Media Dordrecht 2016

**Abstract** We study the Forbush decreases in cosmic-ray intensity from January 2008 to December 2013, covering the minimum between Solar Cycles 23 and 24 and the ascending phase of Cycle 24. We performed a statistical analysis of 617 events and concentrated on three of the most important ones. We used the IZMIRAN database of Forbush effects obtained by processing the data of the worldwide neutron monitor network using the global survey method. The first event occurred on 18 February 2011 with a  $\sim 5\%$  decrease of cosmic rays with 10 GV rigidity, the second on 8 March 2012 with an amplitude of  $\sim 12\%$ , and the third on 14 July 2012 with an amplitude of  $\sim 6\%$ . For these three events, we also studied the events that occurred on the Sun and the way that these affected the interplanetary space, and finally provoked the decreases of the galactic cosmic rays near Earth. We found that each neutron monitor records these decreases, which depend on the cut-off rigidity of the station. We carried out a statistical analysis of the amplitude of the cosmic-ray decreases with solar and geomagnetic parameters.

**Keywords** Solar activity · Forbush decreases · Cut-off rigidity · Neutron monitors

---

✉ H. Mavromichalaki  
[emavromi@phys.uoa.gr](mailto:emavromi@phys.uoa.gr)

D. Lingri  
[dlingri@phys.uoa.gr](mailto:dlingri@phys.uoa.gr)

A. Belov  
[abelov@izmiran.ru](mailto:abelov@izmiran.ru)

E. Eroshenko  
[erosh@izmiran.ru](mailto:erosh@izmiran.ru)

<sup>1</sup> Faculty of Physics, National and Kapodistrian University of Athens, Athens, Greece

<sup>2</sup> Pushkov Institute of Terrestrial Magnetism, Ionosphere and Radio Wave Propagation RAS, Moscow, Russia

# 1. Introduction

Forbush effects (FEs) are short-time (from several hours to several days) decreases in galactic cosmic-ray (GCR) intensity within one to two days that are followed by a slow recovery typically lasting several days. After their discovery by Forbush (1937), the search for their solar sources, responsible interplanetary structures, and physical mechanisms played an important role. These cosmic-ray decreases (Simpson, Babcock, and Babcock, 1955) were generally attributed to solar flares before the beginning of the space age or even later (see, *e.g.* the reviews by Lockwood, 1971 and Venkatesan and Badruddin, 1990). However, with the advent of space coronagraphs in the 1970s and subsequent observations of coronal mass ejections (CMEs) and their interplanetary counterparts (ICMEs), it was realized that CMEs instead of solar flares may be the solar cause of Forbush decreases (FDs). It is known that only some of the observed ICMEs produce Forbush decreases in GCR intensity. Observations using neutron monitor detectors show that the maximum of these depressions can exceed the cosmic-ray intensity by 25 % (Cane, 2000; Belov, 2008). These events occur as the result of strong solar phenomena such as CMEs. The largest FDs are associated with CMEs that are accompanied by shock waves (*e.g.* Cane, 2000; Lockwood, 1971; Mavromichalaki *et al.*, 2005; Papailiou *et al.*, 2012a).

During their travel from the Sun to Earth, CMEs and their corresponding ICMEs interact with galactic cosmic rays that fill the interplanetary space. The leading shock wave of the ICME (if any) and the following ejecta modulate GCRs, which results in a reduced CR intensity (Forbush, 1954). Generally, Forbush decreases are separated into two types. The “non-recurrent decreases” have a sudden onset; the cosmic-ray distribution takes the lowest value in about one day and recovers gradually. Their profiles are asymmetric, and they are associated with transient solar wind disturbances (Cane, 2000). Sometimes an FD appears with a pre-decrease of about 1–3 % that is observed 3–18 hours before the shock arrival at Earth. Then the flux typically pre-increases by about 1–2 %, which shows the incoming decrease and occurs because cosmic rays are reflected on the solar wind shock. After this, the FD is observed, and its amplitude is affected by the area, the velocity, and the strength of the irregular CME magnetic field (Cane and Richardson, 1995; Chauhan *et al.*, 2008). The FD can have one or two steps, depending on the phenomena that have taken place at the Sun (Cane, 2000). FDs that have a gradual onset with a symmetric profile and are called “recurrent decreases”. They are well associated with corotating high-speed solar wind streams (Lockwood, 1971; Xystouris, Sigala, and Mavromichalaki, 2014). These have been found to be greater during the period of high solar activity (Shrivastava, Shukla, and Mishra, 2005).

These cosmic-ray intensity decreases are recorded at Earth by the neutron monitors (NMs) of the worldwide network. The amplitude of the decreases changes with the different cut-off rigidity of each station, which indicates how difficult it is for a cosmic-ray particle to penetrate the Earth’s magnetic field. FDs are more intense in the geomagnetic poles and are not observed simultaneously at all stations over the world; this is a function of the geomagnetic latitude and the position of Earth at the specific moment. It is necessary to emphasize that FDs are independent of atmospheric changes (Cane, 2000), but many of the FDs appear simultaneously with a geomagnetic storm, which is connected with magnetic disturbances in the Earth’s magnetosphere (Belov *et al.*, 2005; Belov, 2008; Chauhan *et al.*, 2008).

It was discovered by Forbush (1954) that the variation of the cosmic-ray intensity correlates inversely with the 11-year variation of the solar activity. This means that at the maximum of the solar activity, cosmic rays present a minimum with a time lag of some months. Most of the FDs driven by CMEs and/or high-speed solar wind streams caused by coronal

holes take place at the minimum of the cosmic-ray intensity and are much larger than those that occur in the low solar activity period (Mavromichalaki and Petropoulos, 1984; Paouris *et al.*, 2012).

In this article, we study the characteristics of the FDs, selected from the database of FEs of cosmic-ray intensity, during the period from January 2008 to December 2013. In Section 2 the sources of all the data used and the data analysis are presented. In Section 3 three specific events are examined in detail, and a further discussion on the relation among the parameters that are responsible for the FDs creation is given in Section 4. Conclusions are summarized in the last section.

## 2. Data Selection and Analysis

We used hourly pressure-corrected values of the cosmic-ray intensity from the neutron monitors of the worldwide network. We selected the well-defined FDs with amplitude  $> 2\%$  that occurred during the time period from 2008 to 2013. We note that the studied period covers the prolonged minimum between the Solar Cycles 23 and 24 up to the end of the first peak of Solar Cycle 24. It is known that Cycle 23 presented many energetic events especially during its declining phase, such as in October–November 2003, in January 2005, and in December 2006. An extended minimum from 2007 to 2010 was followed by strong activity and a short ascending phase that reached a maximum before 2013 and then decreased to have a second activity peak in 2014 (see, *e.g.* Gopalswamy *et al.*, 2014).

The time profile of the daily cosmic-ray intensity values from the Fort Smith neutron monitor (FSMT) for the examined time period is shown in the upper panel of Figure 1. The cosmic-ray data were obtained from the High Resolution Neutron Monitor Database (NMDB) (<http://www.nmdb.eu>). The three more intense FD events that occurred in the examined time period are indicated. Monthly values of the solar flare number and of flares stronger than class M from the GOES satellites (<ftp.ngdc.noaa.gov>) are presented in the middle panels of this figure. The number of halo and partial-halo CMEs from the *Large Angle and Spectroscopic Coronagraph* (LASCO) onboard the *Solar and Heliospheric Observatory* (SOHO) (<http://cdaw.gsfc.nasa.gov>) are also illustrated in the lower panels of this figure. This figure shows very weak solar activity in 2008–2010, although an increased number of flares are observed from 2010 onward with a maximum in 2012.

We studied 617 FEs from January 2008 to December 2013 using the IZMIRAN database. The flares and/or CMEs that may have been associated with them, the interplanetary magnetic field (IMF), the geomagnetic indices, and the sudden storm commencement data (SSC) that took place at the Earth's magnetosphere were obtained from the same database (Belov, 2008; Papailiou *et al.*, 2012b). The IZMIRAN group selected the specific data using the global survey method (GSM), a version of spherical analysis which, by using the cosmic-ray transformation in the Earth's magnetosphere and atmosphere, allows a set of parameters defining the galactic cosmic-ray characteristics to be derived from the neutron monitor network (Belov *et al.*, 2005; Paouris *et al.*, 2012). The IZMIRAN database includes the CR density and anisotropy variations for particles with a rigidity of 10 GV, which is close to the effective rigidity of the particles being registered by the neutron monitor worldwide network (Belov *et al.*, 2005; Belov, 2008; Kryakunova *et al.*, 2013; Paouris *et al.*, 2012). We selected 68 of these events with amplitudes  $> 2\%$  and investigate them here.

For more details about the CMEs associated with these decreases, data from SOHO were used (<http://cdaw.gsfc.nasa.gov>). The solar wind velocity data were taken from the GOES satellites (<ftp.ngdc.noaa.gov>). The neutron monitor data were taken from the High Resolu-

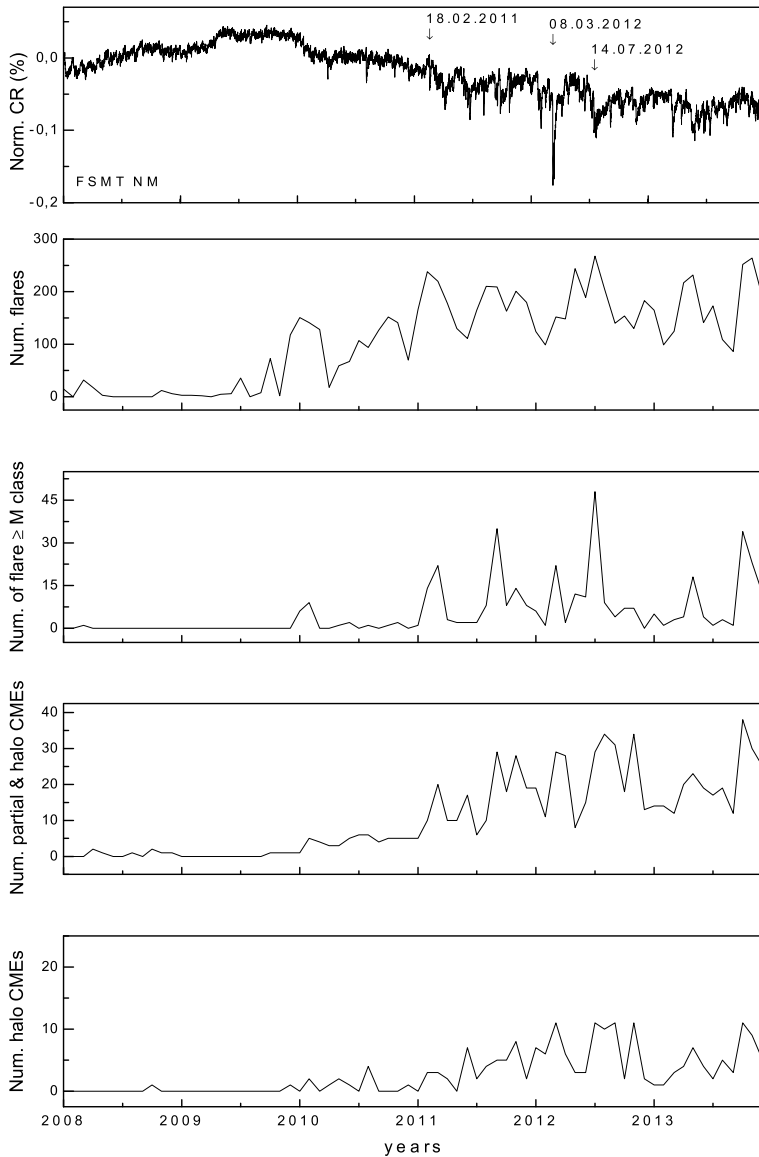


**Figure 1** Time profiles of the cosmic ray intensity (upper panel), of the number of flares *per month* (second panel), of the number of M flares *per month* (third panel), of the number of partial and halo CMEs *per month* (fourth panel), and the number of halo CMEs (bottom panel).

tion Neutron Monitor Database (NMDB) (<http://www.nmdb.eu>), including the Athens Neutron Monitor Station of the University of Athens (ANeMoS) (<http://cosray.phys.uoa.gr>), and the SSC data were obtained from <https://data.noaa.gov/dataset?tags=ssc>. Finally, the geomagnetic indices,  $D_{st}$  and  $K_p$  (<http://wdc.kugi.kyoto-u.ac.jp/>, and <http://www.thesis.lebedev.ru>), were examined. They show the relation between cosmic-ray intensity and geomagnetic activity (Kaushik, Shrivastava, and Rajput, 2005; Papaioannou *et al.*, 2013).

The characteristics of the selected FDs for the time interval January 2008 until December 2013 are given in Table 1 (Lingri *et al.*, 2013). In the first column of this table, we give the date and the arrival time of the solar wind shock wave at Earth (only about half of the selected events started with a shock). It is noted that the primary information for the FDs is based on the SSC time. In the second column we list the amplitude of the observed FDs of the 10 GV cosmic rays obtained by the GSM. In the next two columns, the geomagnetic indices,  $D_{st}$  and  $K_p$ , for the extreme events are shown, and in the fifth column, the maximum intensity of the interplanetary magnetic field is given. In the sixth and seventh columns, we record the maximum velocity of the solar wind when the FD took place and the solar flare associated with the produced FD. Finally, in the last two columns, the date and velocity of the associated CMEs are shown. All data of the columns, such as  $D_{st}$  and  $K_p$  indices, solar wind velocity, and velocity of the CMEs, are the maximum values that appeared around the FD and not at the time of the FD maximum amplitude, which is indicated in the column labeled Ampl.

By examining event by event in Table 1, we see that fast CMEs with velocities greater than  $400 \text{ km s}^{-1}$  seem to be connected with stronger  $D_{st}$  decreases. On the other hand, the slow CMEs produced only small FDs and could not result in a pronounced CR decrease at Earth (Belov *et al.*, 2013). Monthly values of the solar flares and CMEs associated with FDs are presented in the upper and middle panels of Figure 2, respectively. In the lower panel of this figure we present the observable FDs. It is obvious that FDs associated with solar flares and/or CMEs started in 2010, while Forbush effects and solar activity were weak in the period before this.

Moreover, we found that FDs and solar flares are clearly connected, as are CMEs and geomagnetic storms that were moderate ( $-100 \text{ nT} \leq D_{st} \leq -50 \text{ nT}$ ) or intense ( $D_{st} \leq -100 \text{ nT}$ ) and occurred in the magnetosphere. Table 1 shows that most of the storms are not associated with high values of the interplanetary magnetic field. On the other hand, the greater FDs appeared to be related with higher values of the interplanetary magnetic field than the smaller FDs, and this may be because the enhanced magnetic field hinders particles from penetration, which results in FDs with increased amplitude. The presence of a turbulent magnetic field facilitates the particle penetration, which in turn decreases the FD amplitude (Belov, 2008; Badruddin and Kumar, 2015; Parnahaj and Kudela, 2015).

The number of FDs associated with solar flares of different GOES class and their connection with the consequent geomagnetic storms is given in Table 2. For comparison, the data corresponding to the ascending phase of Solar Cycle 23 are given in the same table. Very many FDs in Cycle 24 are associated with solar flares of class M and larger, while in Cycle 23 they are connected with solar flares of class  $> C$  and  $< M$ , although this is not representative because more FDs are associated with M-class flares in Solar Cycle 23 than in Solar Cycle 24. Belov (2008) found that from 1957 to 2006, the FDs with amplitude  $> 3 \%$  corresponded to strong geomagnetic storms (with  $K_p \geq 7$ ) and that FDs with amplitude  $> 12.5 \%$  corresponded to extreme geomagnetic storms. This is not observed in Solar Cycle 24.

As shown in Table 2, the more energetic an associated solar flare on average, the stronger the resulting geomagnetic storm. In our case, there were more geomagnetic phenomena, which were also more intense, in Solar Cycle 23 than in Cycle 24. This occurred because Solar Cycle 23 was a more active cycle and generated many extreme phenomena (Gopalswamy, 2007). Only the X-class flares in Cycle 24 were associated with a greater percentage of intense storms, but this is also because of their very small number in the studied period. The reason that fewer geomagnetic storms occurred in Solar Cycle 24 may be the reduced number of energetic CMEs and the weaker interplanetary magnetic field disturbances. Another possible explanation is the anomalous CME expansion, which is expected to reduce

**Table 1** The selected FDs of the cosmic-ray intensity with their characteristics during 2008–2013. The FDs on 18.02.2011, on 08.03.2012 and on 14.07.2012 studied in more detail in this work.

No.	SSC dd.mm.yyyy, hh:mm (UT)	Ampl. CR 10 GV (%)	$D_{st}$ min (nT)	$K_p$	IMF (nT)	$V_{SW}$ ( $\text{km s}^{-1}$ )	Flares	Date of CME occur. dd.mm.yyyy, hh:mm:ss (UT)	$V_{CMEs}$ ( $\text{km s}^{-1}$ )
1	04.01.2008, 22:50	3.1	−30	4.0	15.9	706	–	02.01.2008, 09:54:04	676
2	26.03.2008, 09:36	2.2	−56	5.0	9.5	676	–	–	–
3	24.06.2008, 20:10	2.2	−29	4.0	13.4	641	–	–	–
4	19.01.2010, 20:00	2.5	−38	4.0	15.5	509	–	–	–
5	05.04.2010, 08:26	2.6	−81	7.7	20.2	783	B7.4	03.04.2010, 10:33:58	668
6	03.08.2010, 17:41	3.3	−67	6.7	17.3	598	C3.2	01.08.2010, 13:42:05	850
7	30.10.2010, 10:13	2.1	−7	2.3	11.7	387	–	26.10.2010, 01:36:05	214
8	12.12.2010, 14:00	2.6	−13	3.7	12.0	660	–	12.12.2010, 02:48:05	543
9	18.02.2011, 01:36	5.2	−30	5.0	30.6	691	X2.2	15.02.2011, 02:24:05	669
10	10.03.2011, 06:45	2.5	−83	5.7	12.0	405	M3.7	07.03.2011, 20:00:05	2125
11	29.03.2011, 16:30	3.1	−2	3.9	14.2	396	–	25.03.2011, 14:36:07	119
12	05.04.2011, 17:00	2.9	−65	5.2	15.2	579	B8.6	–	–
13	04.06.2011, 20:45	3.5	−39	6.4	23.6	556	C3.7	02.06.2011, 08:12:06	976
14	09.06.2011, 18:00	2.6	−31	3.7	10.9	469	M2.5	07.06.2011, 06:49:12	1255
15	17.06.2011, 02:00	2.8	−8	3.8	9.3	546	–	14.06.2011, 06:12:05	571
16	22.06.2011, 03:00	4.1	−25	6.3	10.5	661	C7.7	21.06.2011, 03:16:10	719
17	11.07.2011, 09:00	3.5	−24	3.9	12.6	708	B4.7	09.07.2011, 00:48:05	630
18	05.08.2011, 18:00	4.3	−107	7.8	29.4	611	M9.3	04.08.2011, 04:12:05	1315
19	09.09.2011, 12:43	2.7	−64	5.7	19.3	560	M5.3	06.09.2011, 02:24:05	782
20	17.09.2011, 04:00	2.3	−70	5.3	13.6	549	–	14.09.2011, 00:00:05	408
21	26.09.2011, 12:37	4.4	−101	6.3	34.2	704	M7.1	24.09.2011, 12:48:07	1915
22	05.10.2011, 08:00	2.5	−42	4.3	13.8	470	M1.2	01.10.2011, 09:36:07	448
23	24.10.2011, 18:00	4.9	−132	7.3	24.0	534	–	22.10.2011, 01:25:53	593
24	01.11.2011, 08:00	2.9	−71	4.7	13.0	436	–	27.10.2011, 12:00:06	570
25	22.01.2012, 06:14	3.0	−73	5.0	27.8	451	M3.2	19.01.2012, 14:36:05	1120
26	24.01.2012, 15:04	3.2	−80	4.3	16.7	673	M8.7	23.01.2012, 04:00:05	2175
27	30.01.2012, 16:00	2.6	−17	3.7	10.0	427	X1.7	27.01.2012, 18:27:52	2508
28	31.01.2012, 22:00	2.1	−4	2.3	8.6	433	–	–	–
29	26.02.2012, 21:00	3.5	−47	5.3	14.9	493	–	24.02.2012, 03:46:02	800
30	07.03.2012, 04:21	4.5	−78	6.0	17.1	592	M2.0	04.03.2012, 11:00:07	1306
31	08.03.2012, 11:05	11.7	−143	8.0	23.1	737	X5.4	07.03.2012, 00:24:06	2684
32	12.03.2012, 09:21	5.7	−51	6.3	23.6	727	M8.4	10.03.2012, 18:12:06	1296
33	04.04.2012, 19:00	4.2	−56	4.0	11.7	364	–	–	–
34	30.05.2012, 17:00	3.0	−5	3.7	9.9	444	C3.1	27.05.2012, 05:48:06	725
35	16.06.2012, 20:00	4.6	−86	6.3	40.1	519	M1.9	14.06.2012, 14:12:07	987
36	05.07.2012, 06:00	2.7	3	4.3	10.3	503	C8.2	01.07.2012, 15:36:04	723
37	08.07.2012, 04:00	2.5	−69	6.7	12.3	463	M1.8	04.07.2012, 17:24:04	662
38	14.07.2012, 18:11	6.4	−133	7.0	27.3	667	X1.4	12.07.2012, 16:48:05	885
39	21.07.2012, 16:00	2.2	−21	3.0	13.0	517	M7.7	19.07.2012, 05:24:05	1631
40	26.07.2012, 11:00	2.8	−22	3.7	13.3	417	–	–	–

**Table 1** (Continued)

No.	SSC dd.mm.yyyy, hh:mm (UT)	Ampl. CR 10 GV (%)	$D_{st}$ min (nT)	$K_p$	IMF (nT)	$V_{SW}$ (km s <sup>-1</sup> )	Flares	Date of CME occur. dd.mm.yyyy, hh:mm:ss (UT)	$V_{CMEs}$ (km s <sup>-1</sup> )
41	03.09.2012, 12:14	3.3	-78	5.7	19.8	449	C8.4	31.08.2012, 20:00:05	1442
42	04.09.2012, 22:00	2.8	-68	5.7	15.2	545	C2.9	02.09.2012, 04:00:06	538
43	08.10.2012, 05:15	2.5	-111	6.7	16.3	466	B7.8	05.10.2012, 02:48:00	612
44	09.10.2012, 20:00	2.5	-46	5.0	15.3	551	–	–	–
45	11.10.2012, 13:00	2.8	-91	5.7	12.9	579	–	07.10.2012, 07:36:05	663
46	31.10.2012, 15:39	2.8	-74	4.7	15.8	373	–	27.10.2012, 16:48:05	317
47	12.11.2012, 23:16	4.4	-109	6.3	22.8	454	–	09.11.2012, 15:12:08	559
48	23.11.2012, 20:00	4.2	-42	4.7	15.1	409	M3.5	20.11.2012, 12:00:07	619
49	16.01.2013, 17:00	2.3	-15	4.0	14.7	428	C3.9	–	–
50	17.03.2013, 06:01	4.6	-132	6.7	17.8	725	M1.1	–	–
51	13.04.2013, 05:59	5.3	-7	3.3	12.9	516	M6.5	11.04.2013, 07:24:06	861
52	30.04.2013, 22:54	2.7	-67	5.7	11.1	484	C7.0	28.04.2013, 20:48:05	497
53	05.05.2013, 16:00	2.3	-25	3.3	11.8	548	M5.7	03.05.2013, 18:00:05	858
54	15.05.2013, 07:00	2.9	-32	4.0	11.2	440	X3.2	14.05.2013, 01:25:51	2625
55	25.05.2013, 09:48	2.7	-51	5.0	12.1	777	M5.0	22.05.2013, 13:25:50	1466
56	06.06.2013, 03:00	2.7	-73	5.7	13.4	513	–	04.06.2013, 15:48:06	709
57	23.06.2013, 04:26	5.9	-49	4.3	7.6	697	M2.9	21.06.2013, 03:12:09	1900
58	27.06.2013, 14:38	3.4	-97	5.7	12.5	453	B6.8	25.06.2013, 22:00:05	1139
59	12.07.2013, 16:00	3.0	-51	4.3	16.3	509	–	10.07.2013, 03:12:09	732
60	24.08.2013, 12:00	3.1	-23	2.7	8.8	521	C4.1	22.08.2013, 08:24:05	587
61	03.09.2013, 01:00	3.1	-15	3.3	9.2	472	–	–	–
62	02.10.2013, 02:00	3.3	-75	7.7	22.2	629	C1.2	29.09.2013, 22:12:05	1179
63	14.10.2013, 07:00	2.3	-49	4.3	10.4	546	M1.5	11.10.2013, 07:24:10	1200
64	11.11.2013, 03:00	2.8	-73	4.7	9.6	558	X1.1	10.11.2013, 05:36:05	682
65	22.11.2013, 22:00	2.2	-27	3.3	10.0	372	M1.2	21.11.2013, 01:25:31	775
66	29.11.2013, 01:00	2.8	-12	3.3	11.0	376	–	26.11.2013, 04:24:06	671
67	30.11.2013, 11:00	2.8	-28	3.7	12.6	552	C1.4	27.11.2013, 22:12:27	577
68	14.12.2013, 14:00	5.1	-41	4.0	10.9	600	C4.6	12.12.2013, 03:36:05	1002

the ICME magnetic field strength, and the many halo CMEs during the studied period, which expand into the whole heliosphere (Gopalswamy *et al.*, 2014).

### 3. Dependence of the FD Amplitude on the Cut-off Rigidity

Of the 68 selected FDs presented in Table 1, the three most intense, all in Cycle 24, were considered for a detailed investigation. These events were the result of high solar activity, and we studied them in relation to the cut-off rigidity of the neutron monitor stations.

The Forbush decrease of 18 February 2011 is the first large FD of Solar Cycle 24 and occurred after an X-class flare (X2.2) that occurred on 15 February 2011 at 01:44 UT in the active region (AR) 11158 (<http://umtof.umd.edu/pm/>). The source of this FD was a halo

**Figure 2** Monthly distribution of the solar flares (upper panel) and the halo CMEs (middle panel) and the associated FDs (lower panel) from 2008 to 2013.

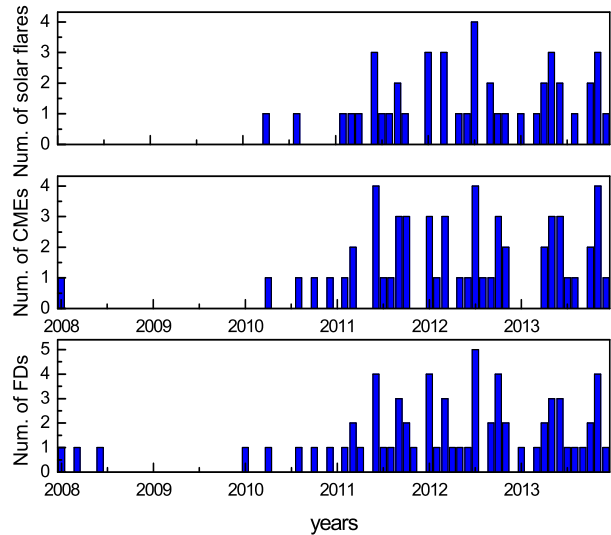


**Table 2** The different GOES-classes of solar flares associated with FDs and the geomagnetic storms (moderate and intense) during the ascending phases of Solar Cycles 23 and 24.

Flare class	Solar Cycle 23 (1999–2001)				Solar Cycle 24 (2010–2013)			
	FDs–flares	GSs ( $D_{st} \leq 50$ nT)	Classification		FDs–flares	GSs ( $D_{st} \leq 50$ nT)	Classification	
			Moderate storm	Intense storm			Moderate storm	Intense storm
B	2	2	1 (50 %)	1 (50 %)	5	4	3 (75 %)	1 (25 %)
C	28	17	7 (41 %)	10 (59 %)	13	5	5 (100 %)	–
M	17	10	4 (40 %)	6 (60 %)	21	12	9 (75 %)	3 (25 %)
X	9	6	2 (33 %)	4 (67 %)	2	3	1 (33 %)	2 (67 %)

CME first recorded by SOHO/LASCO (<http://cdaw.gsfc.nasa.gov>) on 15 February 2011 at 02:24 UT with a velocity of  $669 \text{ km s}^{-1}$ . A sudden storm commenced when the shock arrived at Earth on 18 February 2011 at 01:36 UT (Papaioannou *et al.*, 2013; Lingri *et al.*, 2013). The FD amplitude was 5.2 %, calculated using the GSM for 10 GV particles.

The second Forbush decrease occurred on 8 March 2012 as the result of a series of solar events. As shown in Table 1, this FD is separated into two decreases (7 and 8 March), which prevents us from detecting the exact event that caused them. The CME on 4 March 2012 at 11:00 UT, which was the first CME that caused a disturbance in the interplanetary space, is shown in Table 1. It was followed by three events, one on 5 March at 04:00 UT, and the two others on 7 March, which intensified the disturbance (<http://cdaw.gsfc.nasa.gov>). The greater of them was associated with an X-ray flare (X5.4), which occurred on 7 March 2012 at 00:02 UT in AR 11429 (<http://umtof.umd.edu/pm/>). A CME was first recorded by SOHO/LASCO (<http://cdaw.gsfc.nasa.gov>) on 7 March 2012 at 00:24 UT reaching a great linear speed of  $2684 \text{ km s}^{-1}$ . A little later at 01:30 UT, another CME was produced on the Sun with a velocity of  $1825 \text{ km s}^{-1}$ ; this was associated with an X1.3 flare. As a result of the global disturbance, a severe geomagnetic storm took place when the shock



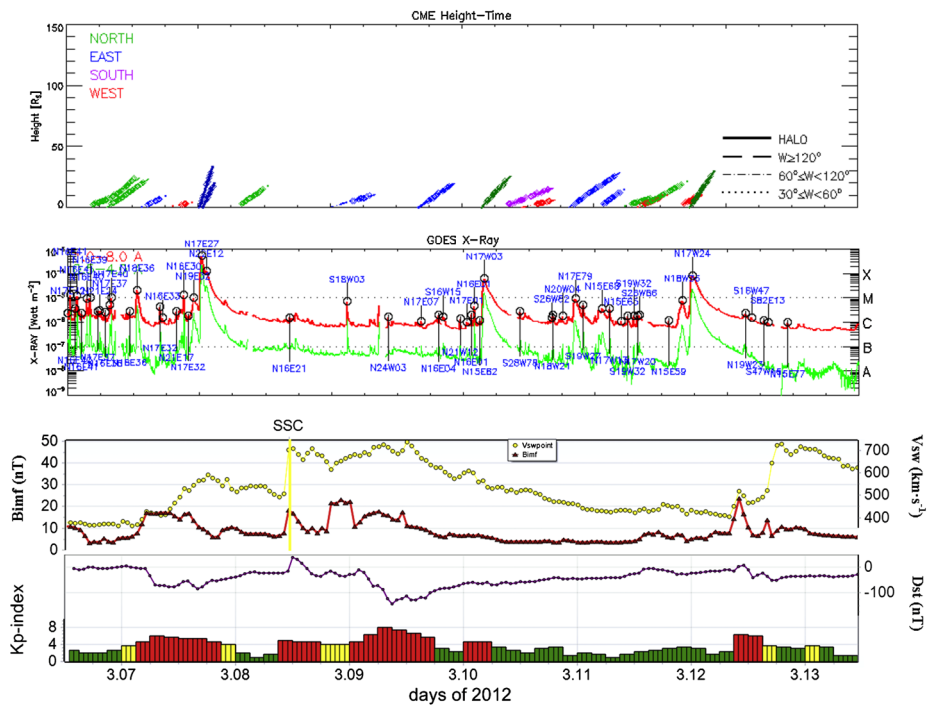


**Figure 3** The CMEs that took place in the period 6–12 March 2012 from SOHO/LASCO (top panel) and the associated flares (second panel) (taken from [http://cdaw.gsfc.nasa.gov/CME\\_list/daily\\_plots/dsthtx/2012\\_03/](http://cdaw.gsfc.nasa.gov/CME_list/daily_plots/dsthtx/2012_03/)), the solar wind velocity and the interplanetary magnetic field (IMF) (third panel), and the variation of the geomagnetic indices  $K_p$  and  $D_{st}$  (bottom panel).

arrived at Earth on 8 March 2012 at 11:05 UT. As a whole, a very complex combination of modulation by several solar sources appeared in this event. The CMEs that took place in the period 6–12 March 2012, the associated flares, the deviation of the solar wind velocity, and the interplanetary magnetic field (IMF) together with the variations of the geomagnetic indices in the same period are presented in Figure 3.

Finally, the third studied event occurred on 14 July 2012 and was associated with an X1.4 flare that occurred on 12 July 2012 at 15:37 UT in AR 11520 (<http://umtof.umd.edu/pm/>). A halo CME was recorded by SOHO/LASCO on 12 July 2012 at 16:48 UT with a plane-of-sky velocity of  $885 \text{ km s}^{-1}$  (<http://cdaw.gsfc.nasa.gov>). An SSC took place in the geomagnetic field, when the shock arrived there on 14 July 2012 at 18:11 UT. The decrease had an amplitude of 6.4 % for cosmic rays of 10 GV. The time profiles of different polar and mid-latitude stations for the three FDs are presented in Figure 4. The hourly values of each NM station are normalized to the mean value of two days before the beginning of each FD.

For these three phenomena, we examined data of the cosmic-ray intensity variations from a number of neutron monitor stations in the northern hemisphere. We obtained the data from the high-resolution Neutron Monitor Monitor Database NMDB (<http://www.nmdb.eu>). A list of these stations with their characteristics is presented in Table 3. The first column shows the name and abbreviation of each station, and the second and third columns give the geographical coordinates and rigidity of each station. The last three columns present the decrease of the cosmic-ray intensity in each event. The neutron monitor stations can be separated according to their geographical coordinates (polar and mid-latitude stations) because the different lo-

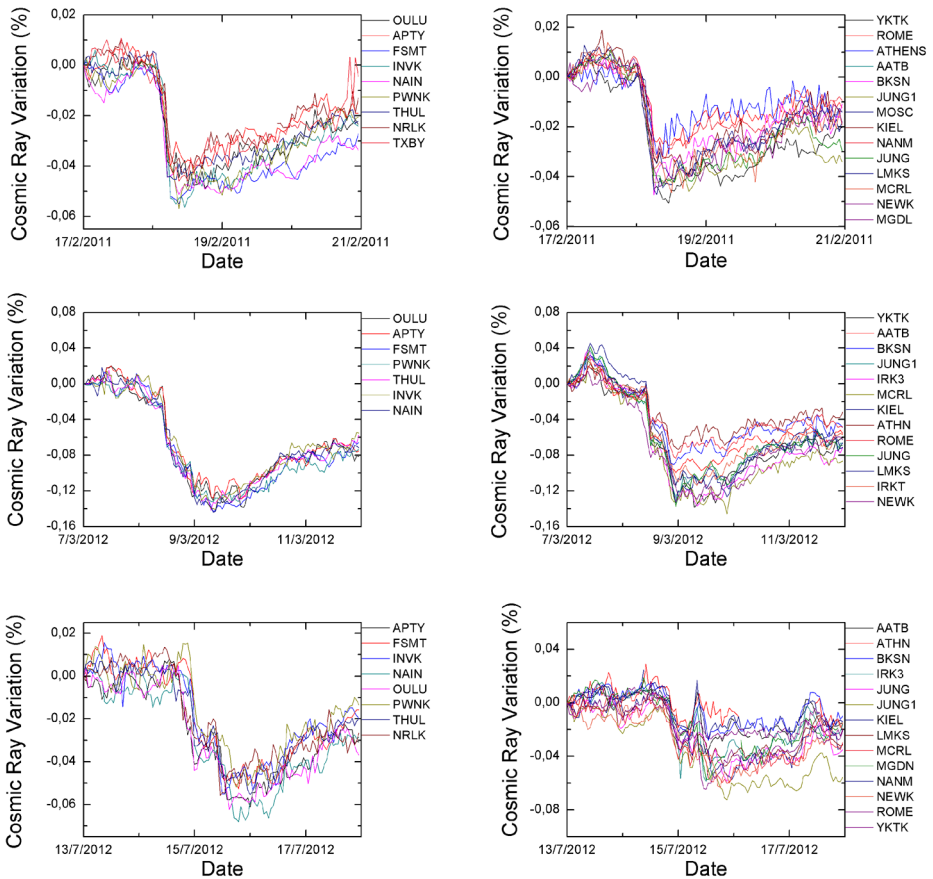


**Figure 4** The FDs on 18 February 2011 (top panels), 8 March 2012 (central panels), and 14 July 2012 (bottom panels) as recorded at northern polar- (left) and mid-latitude (right) stations.

cations of the monitors respond to different energies of the particles, which in turn is related to their cut-off rigidities (Usoskin *et al.*, 2008; Badruddin and Kumar, 2015). By using this categorization, the variations of the CR intensity can be drawn separately for the different geographical latitudes. The three Forbush decreases for the polar- (left panel) and the mid-latitude (right panel) stations are presented in the corresponding upper, middle, and lower diagrams of Figure 4. We see that the decreases of the cosmic-ray intensity in the group of the selected polar stations are greater than in the group of the mid-latitude stations during all these events. This is expected and agrees well with Lockwood (1971).

The dependence of the FDs on the latitude and consequently on the cut-off rigidity of each station can be seen in Figure 5, where the FDs amplitude *versus* the rigidity of each station for the three events is illustrated in the upper, middle, and lower panels of this figure, respectively. We note that the higher the geographical latitude of the station, the greater the FD amplitude. This means that the neutron monitors with a rigidity of up to 6 GV on average are more affected by the solar activity. If the figure had included only these ranges of rigidities, the curve would almost be a straight line. It was shown by Bachelet, Balata, and Lucci (1965) that the latitudinal behavior of cosmic rays at mid-latitude stations is important for the modification of the latitude curves. Results of this work demonstrate that this is also

**Table 3** A list of the neutron monitor stations (first column) with their geographic coordinates (second column) and cut-off rigidities (third column), obtained from the High Resolution Neutron Monitor Database (NMDB, <http://www.nmdb.eu>). The calculated amplitude of the three most intense FDs recorded during the ascending phase of Solar Cycle 24 is illustrated in the next three columns.

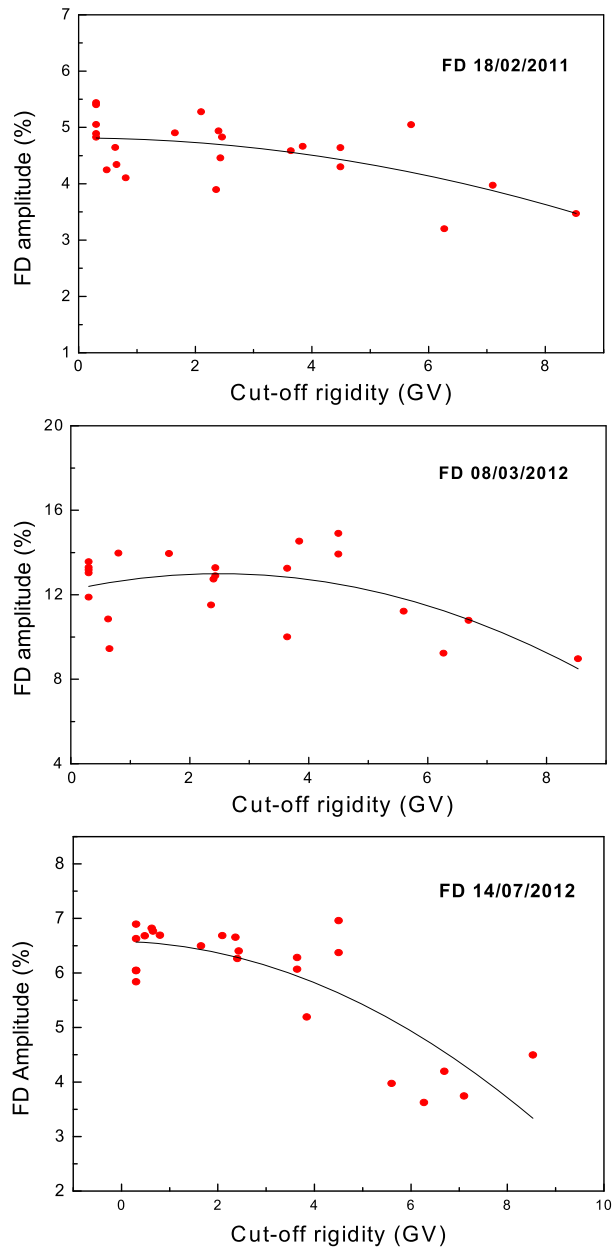
NMDB stations	Station coordinates	Rigidity (GV)	FD amplitude 18/02/2011 (%)	FD amplitude 08/03/2012 (%)	FD amplitude 14/07/2012 (%)
Fort Smith NM, Canada (FSMT)	60.02°N 111.93°W	0.30	5.05	13.03	6.05
Inuvik NM, Canada (INVK)	68.36°N 133.72°W	0.30	5.40	11.89	6.04
Nain NM, Canada (NAIN)	56.55°N 61.68°W	0.30	4.83	13.30	6.89
Peawanuk NM, Canada (PWNK)	54.98°N 85.44°W	0.30	5.44	13.56	6.63
Thule NM, Greenland (THUL)	76.50°N 68.70°W	0.30	4.89	13.17	5.84
Tixie NM, Russia (TXBY)	71.01°N 128.54°E	0.48	4.25	–	6.68
Norilsk NM, Russia (NRLK)	69.26°N 88.05°E	0.63	4.64	10.85	6.82
Apatity NM, Russia (APTY)	67.57°N 33.40°E	0.65	4.34	9.44	6.77
Oulu NM, Finland (OULU)	65.05°N 25.47°E	0.81	4.10	13.97	6.69
Yakutsk NM, Russia (YKTK)	62.01°N 129.43°E	1.65	4.90	13.95	6.50
Magadan NM, Russia (MGDN)	60.04°N 151.05°E	2.10	5.28	–	6.68
Kiel NM, Germany (KIEL)	54.34°N 10.12°E	2.36	3.89	11.52	6.66
Newark NM, USA (NEWK)	39.68°N 75.75°W	2.40	4.94	12.74	6.26
Mobile Cosmic Ray Laboratory, Russia (MCRL)	55.47°N 37.32°E	2.43	4.46	12.90	–
Moscow NM, Russia (MOSC)	55.47°N 37.32°E	2.43	4.83	13.28	6.40
Irkutsk3 NM, Russia (IRK3)	52.47°N 104.03°E	3.64	4.59	10.00	6.28
Irkutsk NM, Russia (IRKT)	52.47°N 104.03°E	3.64	–	13.25	6.07
Lomnický štít, Slovakia (LMKS)	49.20°N 20.22°E	3.84	4.67	14.54	5.19
Jungfraujoch IGY NM, Switzerland (JUNG)	46.55°N 7.98°E	4.49	4.30	14.90	6.37
Jungfraujoch NM64 NM, Switzerland (JUNG1)	46.55°N 7.98°E	4.49	4.64	13.93	6.96
Baksan NM, Russia (BKSN)	43.28°N 42.69°E	5.60	5.05	11.22	3.97
Rome NM, Italy (ROME)	41.86°N 12.47°E	6.27	3.20	9.23	3.62
Almaty NM, Kazakhstan (AATB)	43.14°N 76.60°E	6.69	–	10.78	4.20
Nor-Amberd NM, Armenia (NANM)	40.22°N 44.15°E	7.10	3.97	–	3.74
Athens NM, Greece (ATHN)	37.58°N 23.47°E	8.53	3.47	8.97	4.50

confirmed for the dependence of the FD amplitudes on the cut-off rigidity of each neutron monitor (Figure 5).

#### 4. Statistical Analysis and Results

We performed a correlation analysis of the main parameters of these events such as the amplitude of the FD and the  $D_{st}$  index with other solar and interplanetary parameters such

**Figure 5** FD amplitudes (%) versus the cut-off rigidity of each station for the events on 18 February 2011 (top panel), 8 March 2012 (central panel), and 14 July 2012 (bottom panel).

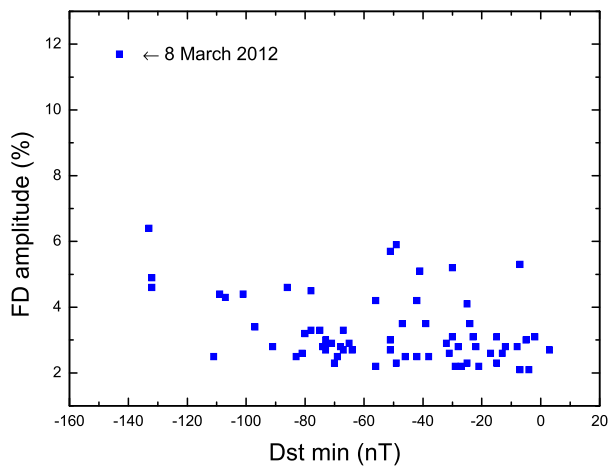


as the associated solar flares and coronal mass ejections, the solar wind ( $V_{\text{SW}}$ ), and the CME plane-of-the-sky velocity ( $V_{\text{CME}}$ ). The obtained linear-fit slopes and the correlation coefficients are given in Table 4.

During Solar Cycle 24, the number of solar flares was lower, and those associated with CMEs were mostly linked to halo CMEs directed at Earth. Only 3 % of the general population of CMEs were full-halo CMEs, and recently, Belov *et al.* (2014) have shown that up to 40 % of them were related to FDs. The FDs that are not associated with flares and CMEs may

**Table 4** Slopes and correlation coefficients obtained from the linear fits of the parameters.

Parameters	Linear-fit slope	Correlation coefficient ( $r$ )
Number of FDs – solar flares	–	0.66
Number of FDs – CMEs	–	0.84
FD amplitude – $D_{st}$ min	$-0.02 \pm 0.01$	0.02
FD amplitude – $V_{SW}$	$0.01 \pm 0.00$	0.40
FD amplitude – $V_{CMEs}$	$0.001 \pm 0.001$	0.20
$D_{st}$ min – $V_{CMEs}$	$-0.01 \pm 0.01$	-0.22
FD amplitude – time interval	$-0.02 \pm 0.01$	-0.13
$V_{SW}$ – time interval	$-2.51 \pm 0.60$	-0.10
$V_{CMEs}$ – time interval	$-10.38 \pm 3.37$	-0.38

**Figure 6** FD amplitudes (%) versus the  $D_{st}$  min (nT) values associated with every event. The event of 8 March 2012 is exceptional.

be caused by corotating solar-wind streams. In Table 1 we show that these FDs appeared during a period of low solar activity, and their amplitude was smaller than those of the others (Mavromichalaki, Vassilaki, and Marmatsouri, 1988; Shrivastava, 2005). When analyzing the relation between the FD amplitude and the  $D_{st}$  index, we find that the amplitudes of all the FDs, except for the event on 8 March 2012, seem to follow a quasi-linear relation with a probable slope of 2 %/100 nT as shown in Figure 6. Certainly, a large FD amplitude is associated with a more negative value of the  $D_{st}$  index, which means strong geomagnetic storms. As has been noted (e.g. Kaushik, Shrivastava, and Rajput, 2005), the  $D_{st}$  index, in general, follows the same decrease pattern as the cosmic-ray particles, while their magnitudes are not proportional to each other. This could be a result of two different generation mechanisms for the FDs and the geomagnetic storms (e.g. Zhang and Burlaga, 1988; Badruddin and Kumar, 2015). However, the  $D_{st}$  index does not seem to have any specific correlation with the velocity of the solar wind in the case of the moderate (left panel of Figure 7) or intense geomagnetic storms (right panel of Figure 7). In addition, the FD amplitude seems to have a linear correlation (0.40) with the solar wind velocity, and the larger amplitudes of FDs appear associated with solar wind velocities higher than  $500 \text{ km s}^{-1}$  (Figure 8). The intense event of 8 March 2012 confirms this result, although we consider it as an exceptional event.

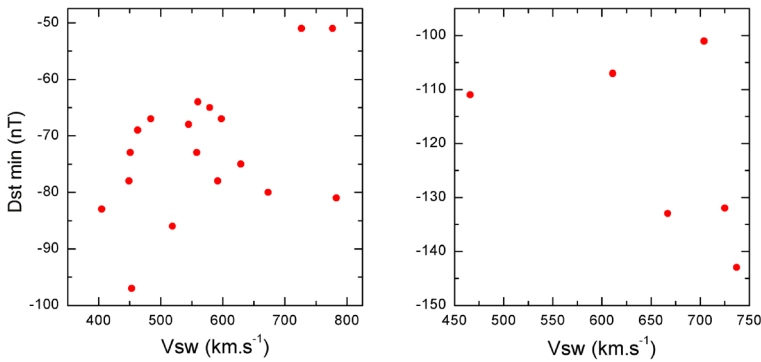
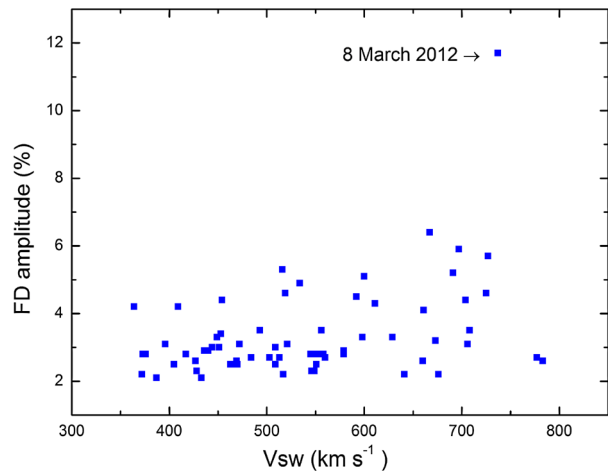


**Figure 7**  $D_{st}$  min values *versus* the velocity of the solar wind for a sub-sample of the FDs (Table 2) associated with moderate (left panel) and intense geomagnetic storms (right panel).

**Figure 8** The relation between the FD amplitudes (in %) *versus* the associated solar wind velocities.



Furthermore, the relation between the FD amplitudes and the  $D_{st}$  index values of the associated storms, with respect to the corresponding CME velocities, seems to have a good correlation, as shown in Table 4 and illustrated in the upper and lower panels of Figure 9. As shown in the lower panel of this figure, most of the CMEs were not related to a large geomagnetic storm. This agrees well with the results of previous works (*e.g.* Gopalswamy, 2007; Shanmugaraju *et al.*, 2015), which found that only about 0.5 % of all halo CMEs are geoeffective with a correlation parameter of the same order of magnitude, as was calculated for the CMEs associated with the events in this figure. But in the figure of the  $D_{st}$  index *versus* the CME velocity, the events on 30 January 2012 and 14 May 2013 do not follow the others either, which might be because Earth was not aligned with the direction of the fast CMEs produced at the Sun on 27 January 2012 and 13 May 2013, respectively. It is still debated whether this event can be considered as a minor ground-level enhancement (GLE) event, while an increase in the high-energy cosmic-ray intensity was recorded at some of the highest latitude stations and at the GOES satellite (Belov *et al.*, 2015).

Finally, we calculated the time interval between the CME appearance and the sudden storm commencement, and we align the relation with other parameters. Dependence of the FD amplitude, the solar wind velocity, and the CMEs velocity on the time interval needed

**Figure 9** FD amplitudes (top panel) and  $D_{st}$  min values (bottom panel) *versus* the velocity of the associated CMEs.

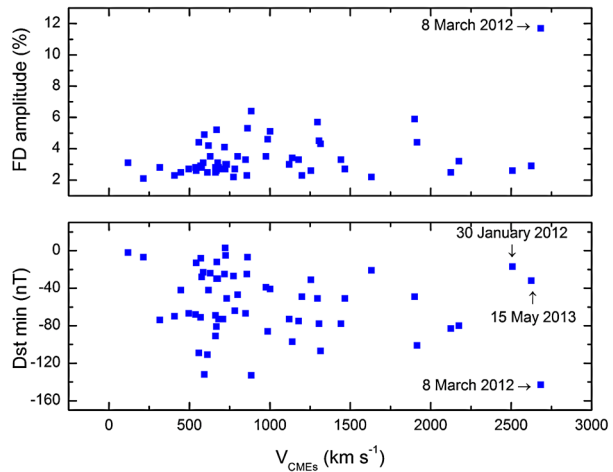
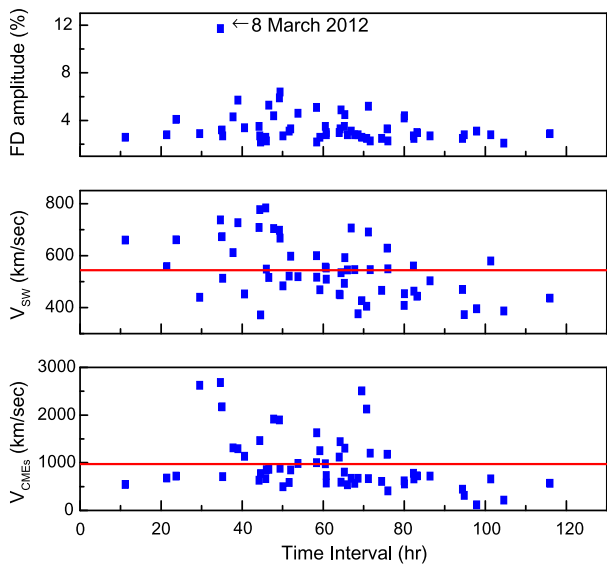


**Figure 10** FD amplitudes (top panel), solar wind velocities (central panel), and CME velocities (bottom panel) *versus* the time interval each CME needs to arrive at Earth and interact with the geomagnetic field. The red horizontal line indicates the mean of the solar wind velocities and of the CMEs.



for the CMEs to arrive at Earth are presented in Figure 10. From this figure, we observe that most of the events that occurred on the Sun and led to a FD greater than 2 %, need a time interval of between 40 and 80 hours to be recorded at Earth. The maximum average velocity of the solar wind in our case was  $(539 \pm 13)$  km s<sup>-1</sup> and the average CME velocity was  $(975 \pm 31)$  km s<sup>-1</sup>. We note that in the studied period the CMEs moved twice as fast as the corresponding ICMEs near Earth. These results agree with those of Belov *et al.* (2014).

## 5. Conclusions

From the extended study of 68 selected FDs (> 2 % for CRs with 10 GV rigidity) out of 617 FEs recorded at neutron monitors between 2008 and 2013, the following conclusions can be drawn:

- The examined time period, covering the minimum between the Solar Cycles 23 and 24 and the ascending phase of the Solar Cycle 24, shows once again that there is a temporal continuity between the solar events and the cosmic ray intensity. When crucial phenomena take place on the Sun, the intensity of the cosmic rays is affected significantly and Forbush decreases are recorded on the Earth's surface, as it is presented in Figures 1 and 2. These FDs are directly associated with fast halo CMEs on the Sun and the shock waves they create, but neither of them is necessarily connected with a solar flare.
- As it is shown in Table 1, the ascending phase of Solar Cycle 24 is characterized by a large number of FDs, but no strong events. Specifically, during the first two years of Solar Cycle 24, only a few relatively strong cosmic ray events occurred, far fewer than during the corresponding period of Cycle 23. As a result the geomagnetic storms that happened were much weaker than those of the previous Solar Cycle 23, with the Dst index to reach values smaller than  $-100$  nT only a few times (Table 2).
- We find that the FDs studied in this article, from 2008 to 2013, were associated with strong flares of class  $\leq M$ , and only three (on 18 February 2011, 8 March 2012, and 14 July 2012) were associated with X-class flares. The greatest one occurred on 8 March 2012 with amplitude of 11.70 % for cosmic rays of 10 GV, obtained by GSM from all neutron monitor stations (Figure 3). These three FDs analyzed in detail (Figure 4) and their amplitude was found to be about the same in the polar neutron monitor stations as in the mid-latitude stations, almost independent of the cut-off rigidity of each station up to 6 GV (Figure 5).
- The statistical analysis of these events in relation with solar and interplanetary parameters (Table 4) showed that the Dst index has a quasi-linear relation with the amplitude of the FDs (Figure 6), but there is no obvious correlation with the solar wind velocity (Figures 6 and 7). On the contrary, the amplitude of the FDs has a linear relation with the solar wind velocity (Figure 8). It is obvious that the most energetic event of March 2012 is an interesting and distinct event, worthy of a more detailed future study.
- In addition, a good correlation was found between the FD amplitudes and the Dst index values, with respect to the corresponding CME velocities (Figure 9). However, most of the CMEs were not related to a large geomagnetic storm. Finally, from the temporal distributions of the FD amplitude, the solar wind velocity, and the CME velocity *versus* the time interval needed for the CMEs to arrive at Earth (Figure 10) we find that the maximum average velocity of the solar wind was  $539 \pm 13$  km s<sup>-1</sup> and the average CME velocity was  $975 \pm 31$  km s<sup>-1</sup>. The time interval varies between 40 and 80 hours as it was recorded at Earth.

In summary, we can say that the FDs of the cosmic ray intensity remain the most important of the cosmic ray events recorded at the ground-based neutron monitors and present many different characteristics in relation with the solar activity parameters during the different phases of the solar cycles. Nowadays, the monitoring and prediction of these events provide important information to the scientific community in the context of space weather studies.

**Acknowledgements** We acknowledge the NMDB database ([www.nmdb.eu](http://www.nmdb.eu)), founded under the European Union's FP7 Program (contract no. 213007) for providing high-resolution cosmic ray data. Thanks are due to ACE/Wind, OMNI, and NOAA data centers for kindly providing the related solar and interplanetary data. Many thanks are also due to the cosmic ray group of the IZMIRAN of the Russian Academy of Sciences for kindly providing the most complete catalog of Forbush decreases. We also acknowledge the anonymous referee for useful comments that significantly improved this work.



## References

- Bachelet, F., Balata, P., Lucci, N.: 1965, *Il Nuovo Cim.* **40**, 250. DOI.
- Badraddin Kumar, A.: 2015, *Solar Phys.* **290**, 1271. DOI.
- Belov, A.V.: 2008, In: Gopalswamy, N., Webb, D.F. (eds.) *Proc. IAU Symposium* **257**, 439. DOI.
- Belov, A.V., Baisultanova, L., Eroshenko, E., Mavromichalaki, H., Yanke, V., Pschelkin, P., Plainaki, C., Mariatos, G.: 2005, *J. Geophys. Res.* **110**, A09520. DOI.
- Belov, A.V., Abunin, A., Abunina, M., Eroshenko, E., Papaioannou, A., Mavromichalaki, H., Oleneva, V., Yanke, V., Gopalswamy, N., Yashiro, S.: 2013, In: *ESA Space Weather Week 10*, Seq. 13/A2920697, 152.
- Belov, A.V., Abunin, A., Abunina, M.A., Eroshenko, E., Oleneva, V., Yanke, V., Papaioannou, A., Mavromichalaki, H., Gopalswamy, N., Spapiro, S.: 2014, *Solar Phys.* **289**, 3949. DOI.
- Belov, A.V., Eroshenko, E.A., Kryakunova, O.N., Nikolayevskiy, N.F., Malimbayev, A.M., Tsepakina, I.L., Yanke, V.G.: 2015, *Bull. Russ. Acad. Sci., Phys.* **79**, 561. DOI.
- Cane, H.: 2000, *Space Sci. Rev.* **49**, 55. DOI.
- Cane, H., Richardson, I.G.: 1995, *J. Geophys. Res.* **100**, 1755. DOI.
- Chauhan, M.L., Shrivastava, S.K., Richharia, M.K., Jain, M., Jain, A.: 2008, In: *Proc. 30th ICRC*, **1**, 307.
- Forbush, S.E.: 1937, *Phys. Rev.* **51**, 1108. DOI.
- Forbush, S.E.: 1954, *J. Geophys. Res.* **59**, 525. DOI.
- Gopalswamy, N.: 2007, *The High Energy Solar Corona: Waves, Eruptions, Particles, Lecture Notes in Physics* **725**, Springer-Verlag, Berlin, Heidelberg, 139.
- Gopalswamy, N., Akiyama, S., Yashiro, S., Xie, H., Maekelae, P., Michalek, G.: 2014, *Geophys. Res. Lett.* **41**, 2673. DOI.
- Kaushik, S.C., Shrivastava, P., Rajput, H.M.: 2005, In: *Proc. 29th ICRC*, vol. 2, 151.
- Kryakunova, O., Tsepakina, I., Nikolayevskiy, N., Malimbayev, A., Belov, A., Abunin, A., Abunina, M., Eroshenko, E., Oleneva, V., Yanke, V.: 2013, *J. Phys. Conf. Ser.* **409**, 012181. DOI.
- Lingri, D., Papahliou, M., Mavromichalaki, H., Belov, A., Eroshenko, E., Yanke, V.: 2013, In: *Proc. 11th Hel.A.S Conf.* [http://www.helias.gr/conf/2013/posters/S\\_1/mavromichalaki\\_2.pdf](http://www.helias.gr/conf/2013/posters/S_1/mavromichalaki_2.pdf).
- Lockwood, J.A.: 1971, *Space Sci. Rev.* **12**, 658. DOI.
- Mavromichalaki, H., Petropoulos, B.: 1984, *Astrophys. Space Sci.* **106**, 61. DOI.
- Mavromichalaki, H., Vassilaki, A., Marmatsouri, E.: 1988, *Solar Phys.* **115**, 345. DOI.
- Mavromichalaki, H., Papaioannou, A., Petrides, A., Assimakopoulos, B., Sarlanis, C., Souvatzoglou, G.: 2005, *Int. J. Mod. Phys. A* **20**, 6714. DOI.
- Paouris, E., Mavromichalaki, H., Belov, A., Gushchina, R., Yanke, V.: 2012, *Solar Phys.* **280**, 255. DOI.
- Papailiou, M., Mavromichalaki, H., Belov, A., Eroshenko, E., Yanke, V.: 2012a, *Solar Phys.* **276**, 337. DOI.
- Papailiou, M., Mavromichalaki, H., Belov, A., Eroshenko, E., Yanke, V.: 2012b, *Solar Phys.* **280**, 641. DOI.
- Papaioannou, A., Belov, A., Mavromichalaki, H., Eroshenko, E., Yanke, V., Asvestari, E., Abunin, A., Abunina, M.: 2013, *J. Phys. Conf. Ser.* **409**, 012202. DOI.
- Parnahaj, I., Kudela, K.: 2015, *Astrophys. Space Sci.* **359**, 35. DOI.
- Shanmugaraju, A., SyedIbrahim, M., Moon, Y.-J., Mujiber Rahmanm, A., Umapathym, S.: 2015, *Solar Phys.* **290**, 1417. DOI.
- Shrivastava, P.: 2005, In: *Proc. 29th ICRC*, **1**, 355.
- Shrivastava, P., Shukla, R., Mishra, R.: 2005, In: *Proc. 29th ICRC*, vol. 1, 335.
- Simpson, J.A., Babcock, H.W., Babcock, H.D.: 1955, *Phys. Rev.* **98**, 1402. DOI.
- Usoskin, I.G., Braun, I., Gladysheva, O.G., Hörandel, J.R., Jämsén, N.T., Kovaltsov, G.A., Starodubtsev, S.A.: 2008, *J. Geophys. Res.* **113**, A07102. DOI.
- Venkatesan, D., Badruddin: 1990, *Space Sci. Rev.* **52**, 121. DOI.
- Xystouris, G., Sigala, E., Mavromichalaki, H.: 2014, *Solar Phys.* **289**, 995. DOI.
- Zhang, G., Burlaga, L.F.: 1988, *J. Geophys. Res.* **93**, 2511. DOI.